We are IntechOpen, the world's leading publisher of Open Access books
Built by scientists, for scientists

6,100
Open access books available

149,000
International authors and editors

185M
Downloads

Our authors are among the

154
Countries delivered to

TOP 1%
most cited scientists

12.2%
Contributors from top 500 universities

CLARIVATE ANALYTICS
BOOK CITATION INDEX
INDEXED

WEB OF SCIENCE™

Selection of our books indexed in the Book Citation Index
in Web of Science™ Core Collection (BKCI)

Interested in publishing with us?
Contact book.department@intechopen.com

Numbers displayed above are based on latest data collected.
For more information visit www.intechopen.com

Chapter

Principles of Diagnosing the Technical Condition of the Bearings of the Gas Turbine Engine Supports Using Rhythmogram and Scatterogram

Dmitry Balakin, Vitaly Shtykov, Alexey Zubko,

Shalimova Elena Vladimirovna and Zayed Saleh Salem Ali

Abstract

The possibility of using a rhythmogram and a scatterogram for bearings of diagnosing a gas turbine engine and its components is discussed. Rhythmogram and scatterogram evaluate the quasi-periodicity of the technical system of a gas turbine engine. Rhythmogram and scatterogram were obtained using the method developed by us for processing quasi-periodic pulse signals. The method is based on the principles of the theory of optimal filtering, the theory of wavelet transform, and the Hermite transform. The wavelet transform is considered as a cross-correlation function. The Gauss-Hermite functions are used as the basis for wavelet analysis. The effectiveness of the diagnostic method is demonstrated by the example of the operation of the bearing supports of a gas turbine engine and the engine as a whole.

Keywords: gas turbine engine, rotor bearings, hermit transform, wavelet transform, optimal filtering, rhythmogram, scatterogram

1. Introduction

Most machines and mechanisms as part of their design have rotating elements that transfer the load to the stator through bearings. Structurally, they can be of various types, and the possibility of functioning of the entire device depends entirely on their performance.

Even higher requirements are placed on bearings that are used in the rotor bearings of aircraft gas turbine engines. With a small mass, they must transmit large variable loads and work with high speeds of movement of the contacting parts of their design.

When designing rotor systems of gas turbine engines (GTEs), many years of experience in the development of such structures are taken into account, and computational simulations and their verification are carried out based on the results of various integrated tests. Such methods of calculation and full-scale experiment take

into account and repeatedly check the influence of a large number of external and internal factors that can drastically reduce the duration of uptime of engines.

At the same time, despite the progress made in the field of computer design, simulation, and testing, it will never be possible to take into account the entire set of product states due to the manifestation of all possible combinations of values of the influence of various factors that may arise during long-term operation of engines.

Given the importance of ensuring long-term trouble-free operation of the bearings of the rotor systems of GTE, the most promising trend can be considered as the provision of such a design with a developed monitoring and diagnostic system. It should provide a permanent opportunity to determine the technical condition of the bearings in all operating modes of the engine and issue warnings to the crew in cases of rapidly developing damage to their parts.

In view of the importance and complexity of this issue, we have set a goal to provide the possibility of diagnosing the inter-rotor bearing of the GTE turbine support by developing nontraditional diagnostic methods.

Modern methods and algorithms are required not only to diagnose existing defects but also to detect changes in the state of the system before an emergency occurs. In this direction, it is worth noting the works of domestic scientists: Barkov A.V., Barkova N.A. [1].

For technical diagnostics of nonstationary systems, a wavelet transform is used, which makes it possible to adapt to the local properties of the signal, which increases the efficiency of diagnostics. This is evidenced by the works of scientists such as Adewusi S. A. [2], Chancey V. C., and [3], Peng Z. [4]. Wavelet the transform gives a time-frequency representation of the signal, thereby avoiding many of the problems that arise when using the Fourier transform. The impulses of the system under study can have an arbitrary shape; therefore, to describe them, it is necessary to use orthogonal functions. The most popular orthogonal wavelets are the Haar and Daubechies wavelets [5]. They have a number of limitations and disadvantages. Haar wavelets poorly describe smooth functions, and Daubechies functions have an asymmetric form, which narrows the area of their practical use. Thus, with the help of classical wavelets, it is not possible to take into account all the features of the pulse shape, which affects the quality of diagnostics. In this regard, when processing real signals, it is necessary to construct a "mother" function based on a discrete record of the signal, and this is absent in the classical interpretation of the wavelet transform.

This goal can be achieved by solving the following tasks:

- development of a diagnostic method based on new principles for obtaining and analyzing diagnostic information;

- obtaining diagnostic signs of an early manifestation of a developing malfunction and developing a diagnostic model of an inter-rotor bearing.

2. Theoretical foundations of the processing method

The most popular diagnostic methods bearings can be divided into two broad categories: spectral methods and time methods.

In the general case, the analysis algorithm based on the spectral method is as follows: using the properties of the Fourier transform, the signal spectrum is calculated:

$$F(\omega) = S_0(\omega) \sum_{n=0}^{N} \exp(-j\omega\tau_n), \qquad (1)$$

where $S_0(\omega) = \int_{-\infty}^{\infty} S(t) \exp(-j\omega t)dt$ _ bearing signal spectral density ($S(t)$). The calculation $F(\omega)$ is based on statistical properties τ_n. The parameter τ_n is a random value that characterizes the quasi-periodicity of the process under study, and the index n shows the pulse number. As a rule, when analyzing the bearing signals by the method (1), it is assumed that process is stationary, so its properties, determined in short time intervals, do not change from the interval to the interval. Thus, $\tau_n = nT$ which is the period of the impulses. Using spectral methods, we can confidently detect defects that are characterized by the occurrence of a periodic component. This is the wear of the rolling bearings, the weakening of mechanical joints in the engine, and much more. Spectral methods include methods based on the analysis of the broadband energy spectrum [6], the frequency component [7], the spectrum of the envelope signal [8], and the window conversion of Fourier [9].

Another direction in technical diagnosis is temporary analysis. Due to this, it can find some characteristics that are difficult to identify using spectral analysis. For example, according to the parameters of a temporary signal, you can detect the number of shock pulses, which in the spectrum may not be distinguishable due to the presence of interference and noise [10].

The disadvantages of classical methods of spectral and temporary processing include that they give only the general condition of the system under study. In addition, classical methods significantly reduce their effectiveness in the analysis of nonstationary processes, which complicates the assessment of dynamic parameters (quasi-periodicity), which means they cannot effectively give a forecast about how the system will behave in the future.

A method is proposed that occupies an intermediate position between spectral and temporary methods and is based:

1. On the main properties of the transformation of the Hermit;

2. On the main properties of the wavelet transformation;

3. On the classical theory of optimal filtration.

Thanks to the use of the basic properties of the wavelet transformation (scaling and localization), the method allows us to adapt to the local features of the bearing signal. As basic functions, the method uses the functions of the Gauss-Hermite (FGH), which are defined in the transformation of the Hermit [11]. The undoubted advantage of the FGH is that they are orthogonal in both the temporary and frequency area, which allows them to adapt them not only to the form of the signal in time, but also to its frequency spectrum. It is also worth noting that the method works throughout the sample of the signal under study, which increases its effectiveness but affects the calculation speed. The stability of the method for noise increases due to the fact that it is based on the principles of optimal filtration. At the output of the method, we have a cross-correlation function, according to which the dynamics of the pulse is evaluated (assessment of quasi-periodicity or τ_n) by measuring the distance between

the peaks. For clarity and information content, this procedure can be replaced with an assessment of the rhythmogram of the process under study. The rhythmogram is an apparatus for evaluating quasi-revisionism adopted in the medical field. The rhythmogram reflects the variability of the heart rhythm. Thus, the use of a rhythmogram to assess the state of the bearing is a new field in the diagnosis of technical systems.

2.1 Mathematical description of the method

The mathematical procedure for processing the signal of the bearing can be described by the following scheme:

The input digital signal $S_{in}(t_k)$ (signal after sampling and quantization), obtained from the vibration sensors, changes with a reference signal $\tilde{S}_{ptrn}(t_k, m)$. A reference signal is a fragment of a record $S_{in}(t_k)$, the dynamics of which we want to trace. A reference signal can be interpreted as a defect or a useful signal, the choice depends on the objectives of the study. A reference signal can be built in the following expression:

$$\tilde{S}_{ptrn}(t_k, m) = \frac{1}{\sqrt{2^m}} \sum_{q=0}^{Q} W(q, q_{cf}) A_q(m) \Psi_q(t_k, m) \qquad (2)$$

The main computing element (2) is the calculation, which is based on the transformation of the Hermit or FGH and the discrete wavelet transformation:

$$A_q(m) = \left(q! 2^q \sqrt{\pi}\right)^{-1/2} \sum_{k=-K}^{K} S_{ptrn}(t_k) \Psi_q(t_k, m), \qquad (3)$$

where $S_{ptrn}(t_k)$ is the vector of samples of the selected fragment (or the standard is a fragment from $S_{in}(t_k)$), $t_k = \Delta t \cdot k$, Δt is the sampling step, $K = N_{ptrn}/2$, N_{ptrn} is the duration of the selected fragment in samples, $k = -K, . -1, 0, 1, .. K$, borders on $\Delta t = 3/K$, time by level ± 3, $\Psi_q(t_k, m)$—FGH q—FGH order, m is the scale parameter (similar to the scale parameter in the wavelet transform). In fact, (3) is the decomposition of a fragment $S_{ptrn}(t_k)$ in space $\Psi_q(t_k, m)$. Gauss-Hermite functions have the following mathematical notation:

$$\Psi_q(t_k, m) = H_q\left(\frac{t_k}{2^m}\right) \exp\left(-0.5\left(\frac{t_k}{2^m}\right)^2\right), \qquad (4)$$

where $H_q\left(\frac{t_k}{2^m}\right)$—Hermite q—order polynomial.

Then, (2) is the inverse Hermite transform, and the reproduction accuracy $S_{ptrn}(t_k)$ is determined by the expression:

$$Er(m, q) = \frac{\sum_{k=-K}^{K} \left(\frac{1}{\sqrt{2^m}} \sum_{q=0}^{Q} W(q, q_{cf}) A_q \Psi_q(t_k, m) - S_{ptrn}(t_k)\right)^2}{\sum_{k=-K}^{K} S_{ptrn}(t_k)^2} 100\%, \qquad (5)$$

where $W(q, q_{cf})$ is the smoothing filter in FGH space. When the series is truncated in FGH space, the reference signal has oscillations, and this effect is analogous to the

"Gibbs phenomenon" in harmonic analysis. To weaken it, you can use low-pass filtering in the FGH space, based on well-known approximations of the frequency characteristics: Gauss, Butterworth, and Bessel.

The error $Er(m, q)$ can be set by the researcher and is determined by the maximum FGH order—Q .

The key feature of the signal according to (2) is that it is built from a real discrete record of the signal, so we can take into account any local features of the process under study.

In accordance with the scheme of **Figure 1**, the next operation is the integration or calculation of the correlation integral. The correlation integral is defined in the theory of optimal filtering and searches for similar fragments $\tilde{S}_{ptrn}(t_k, m)$ is the process under study $S_{in}(t_k)$. In this paper, the correlation integral is built on the basis of the wavelet transform:

$$R_{out}(t_n, m) = \sum_{k=0}^{N} S_{in}(t_k)\tilde{S}_{ptrn}(m, t_k - t_n), \qquad (6)$$

where N is the maximum number of samples in the signal $S_{in}(t_k)$. As you can see, with a large number of readings, calculation (6) is computationally labor-intensive. Therefore, it makes sense to move from spatial integration in the time domain to multiplication in the frequency domain or matched filtering. Then the scheme of **Figure 1** can be transformed into the following form (**Figure 2**):

The signal goes directly to the matched filtering (*MF*) block. With matched filtering, an increase in the detection rate is associated with the following circumstances:

1. the spectral image of the Gauss-Hermite functions is known;

2. the orthogonal basis of the Gauss-Hermite functions in space-time corresponds to the orthogonal basis of the Gauss-Hermite functions in the frequency domain;

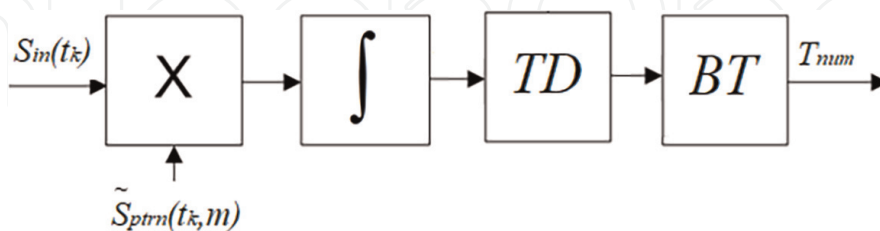3. when calculating in the spectral region, you can use the fast Fourier transform procedure.

Figure 1.
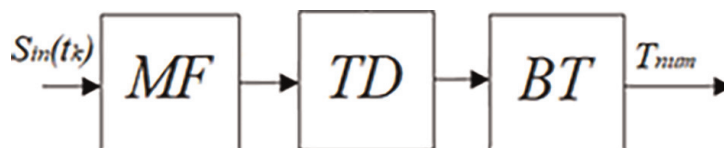*Block diagram of the processing method in the temporary area.*

Figure 2.
Flowchart of the processing method in the time-frequency domain.

It was obtained [12] the transmission coefficient of the filter that selects a fragment of the signal, consisting of a set of features:

$$\dot{K}(f_n, m) = \sum_{q=0}^{Q} j^q \sqrt{\frac{\sqrt{\pi}}{q! 2^{q-1}}} \exp\left(-0,5(2^m)^2 f_n^2\right) H_q(2^m f_n), \qquad (7)$$

where $f_n = n/N\Delta t, n = 0,1,\dots N-1$.

The signal after matched filtering the cross-correlation function enters the threshold device (TD), where, based on a priori statistical information, peaks exceeding a certain threshold value are selected. The median value can be used as a threshold. After threshold processing, the resulting one enters the block of transformation (BT), at the output of which we have the rhythmogram of the process (T_{num}).

Due to the fact that the principles of the wavelet transformation are incorporated in the processing method, the rhythmogram can be refined by varying the scale parameter or the filter band (7):

$$F(t_k, m) = \sqrt{E_s} - \left| \frac{1}{2\pi\sqrt{a}} \sum_{n=0}^{N-1} \dot{S}_{in}(f_n) \dot{K}_q(f_n, \; m) \exp\left(\frac{j2\pi f_n t_k}{N}\right) \right|, \qquad (8)$$

As a result, a functional or a surface is formed, on which there are many extrema (minimums) corresponding to the number of reference signals in the process under study. The processing process is reduced to solving a multi-extremal problem. This problem is solved using the steepest descent method, where a priori information about the rhythm of the system under study can serve as starting points. However, in real problems, such information is not always available. Therefore, as a starting point for the steepest descent algorithm, it is advisable to use the coordinates of the maxima of the cross-correlation function determined at an early stage without changing the scale parameter. As a result of such processing, we obtain refined information about the location of the reference signal and, consequently, a more accurate process dynamics or rhythmogram.

2.2 Signal processing without a priori information

The records of three signals (S_1, S_2, S_3) are shown in **Figure 3**. The sample size is 30,000 readings. In accordance with the considered theory, it is necessary to isolate the standard from the signal under study. The standard is a fragment of the recording, the dynamics (rhythm) of which we want to trace throughout the entire time of the study. The standard reflects the distinctive features of the waveform, which can mean both the correct operation of the device, and, conversely, a faulty one. The choice of standard should be carried out taking into account the opinion of a specialist or an expert in the field of diagnostics. Since we do not have a priori information on the characteristic features of the signal, we will conduct a preliminary spectral analysis of the signals to select the standard.

Take the value of the sampling frequency equal to 1. Then, for a sample of 30,000 samples, the frequency step in the spectral region will be 1/30,000 rel. units. The recording spectra are shown in **Figure 4**. The figure shows that the maximum frequency components in the signal spectra are concentrated in the range of approximately 0.015–0.02 rel. units, which corresponds to approximately 50–70 samples in the signal record.
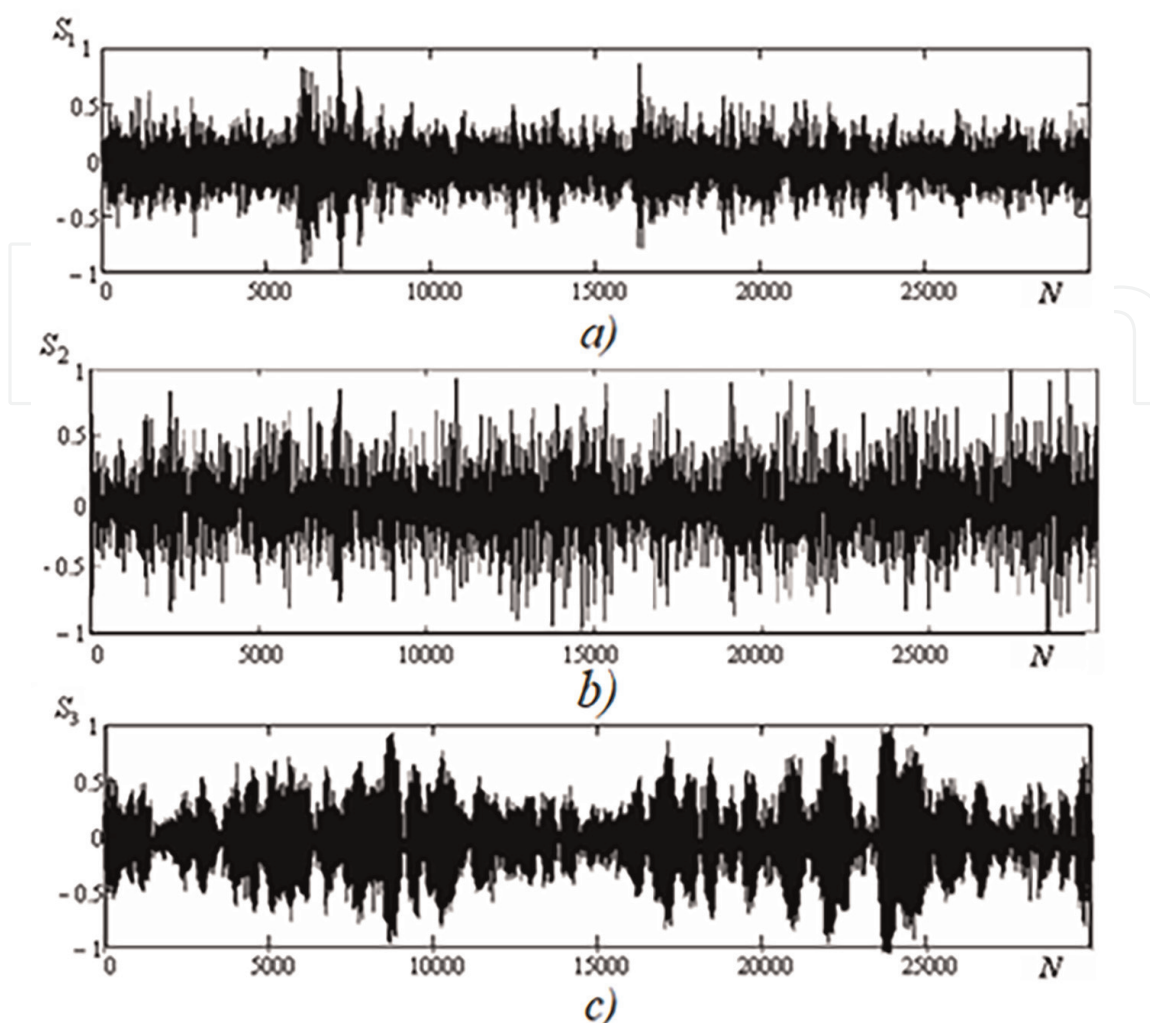
Figure 3.
Recordings of vibration signal of bearings: N—count number.

The ideal mechanism functions cyclically, which is determined by the characteristic spectral component. In the discrete spectrum of the signal of such a mechanism, the reciprocal of the period has a maximum value. In real records, the spectrum is blurred (**Figure 4**), but its maximum can be identified with the average pulse repetition period.

After analyzing the spectra, it can be established that the signal S_2 is a faulty operation of the bearing, since many spectral peaks are observed in the spectrum. Bearing signals S_1 and S_2 are of the greatest interest due to the fact that it is impossible to say for sure from the spectral pattern whether they are in good order or not. Let us choose a signal fragment from the record as a reference, since its main spectral components are present both in the signal spectrum and in the signal spectrum.

After analyzing the record, a fragment (from 6020 to 6080 samples) was selected, shown in **Figure 5**, since similar waveforms occur throughout the entire signal record.

In **Figure 5**, characteristic fragments with a duration of approximately 50–70 samples are clearly visible. The next stage of processing is the construction of a support function (SF) based on FGH. In essence, SF is a mirror image impulse response of a complex quasi-matched filter (7). As a result of multiplying the complex conjugate transfer coefficient of the quasi-matched filter and the spectrum of the signal under study, after the inverse Fourier transform, we obtain the cross-correlation function, fixing its maxima, we can build a rhythmogram.
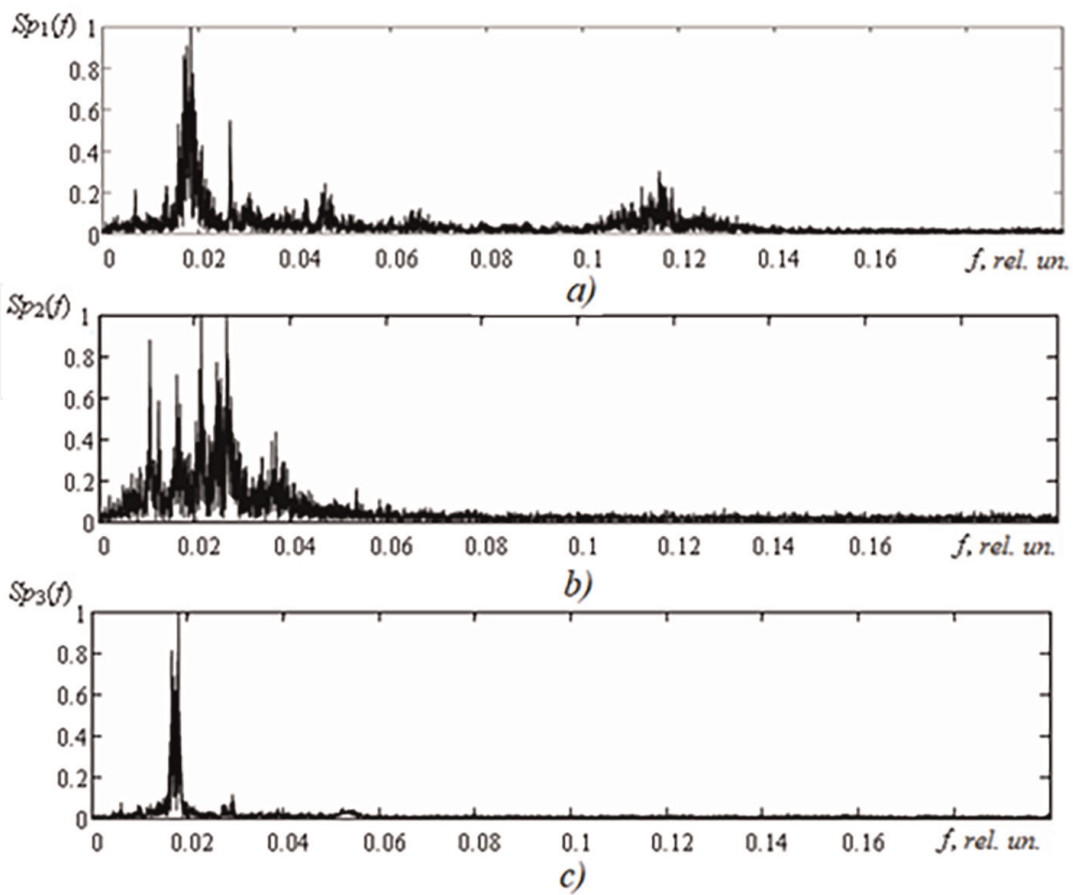
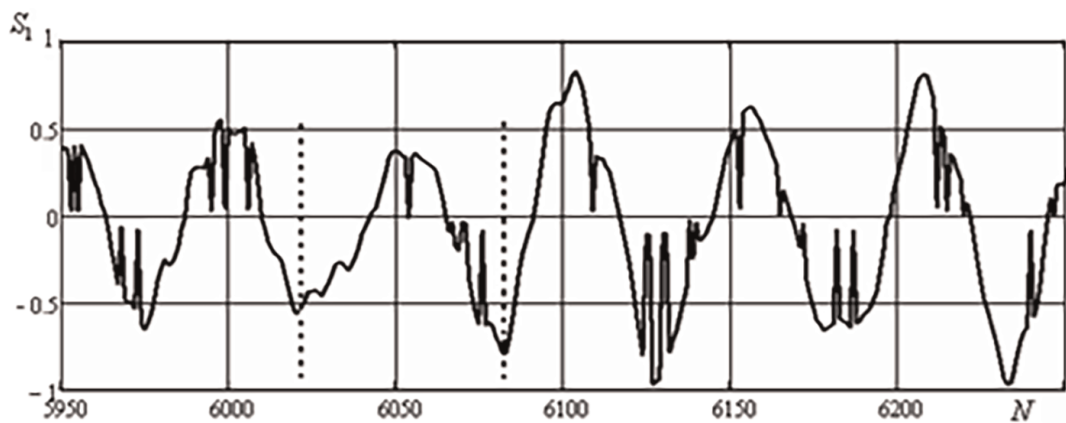**Figure 4.**
Spectra of the studied signals.

Figure 5.
Fragment of the record S_1.

The position of the extrema of cross-correlation function can be refined by varying the scale parameter when constructing the filter (8). Thus, the problem of diagnosing a system is reduced to solving a multi-extremal problem, since the cross-correlation function is a complex surface with many local maxima. From a methodological point of view, it is more convenient to look for local minima. This transition can be made using the Cauchy-Bunyakovsky inequality (**Figure 6**).
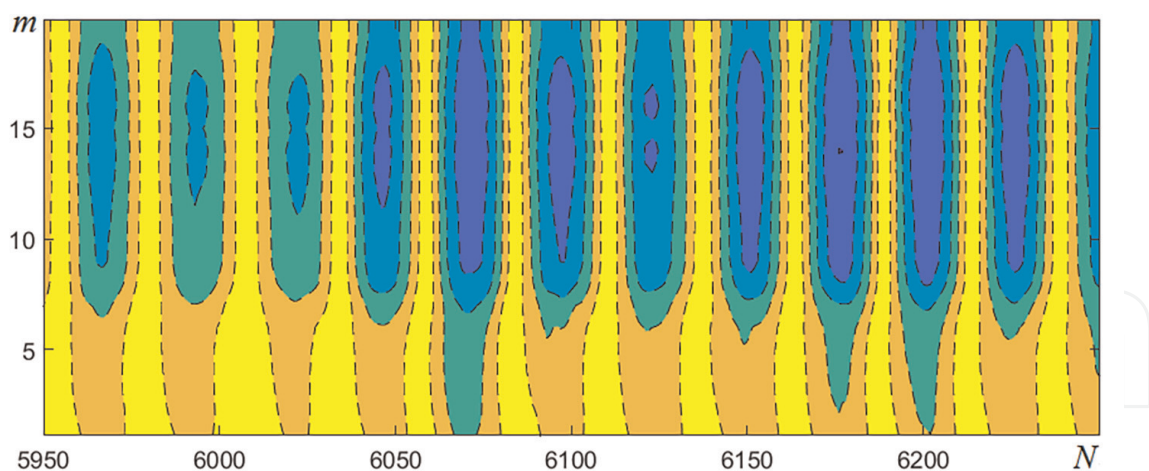
Figure 6.
Topographic picture of the cross-correlation function of a signal S_1 fragment with a variation of the scale parameter.

Such a procedure (**Figure 6**) resembles the process of scale variation in the wavelet transform. The key difference between the two processing approaches is that at the output of the method under consideration, we have the cross-correlation function that allows us to estimate the degree of similarity of the SF and the reference, and with wavelet processing, the spectral distribution. The position of the minima of the obtained surface can be found, for example, by the steepest descent method.

As a result of such processing, we have rhythmograms and scatterograms.

To construct the rhythmogram, the cross-correlation function was subjected to threshold processing. The processing results are shown in **Figure 7**.

When constructing the diagram, the minimum positive value from the set of maxima of the cross-correlation function signal S_1 was taken as the threshold.

Rhythmograms look like a random process with an average value. It is approximately equal to 50 samples and gives an estimate of the average period of the processed signals.

Rhythmogram surges indicate deceleration (upsurges) or acceleration (downsurges) of the mechanism. Upsurges commensurate with the average value of the rhythmogram indicate that the algorithm skipped a cycle due to the fact that the maximum cross-correlation function does not exceed the set threshold. There are few such outliers in **Figure 7a** and **c**, while there are quite a lot of them in Figure 57b. In the presence of noise, downward spikes may appear, commensurate with the average value of the rhythmogram, due to the appearance of false maxima. There are no such outliers in **Figure 7**.

Preliminary visual analysis suggests that the bearings, the signals of which are shown in **Figure 1a** and **c**, are in good condition, and the bearing with the signal S_2 has a defect. Let us confirm these preliminary considerations with quantitative estimates.

The rhythmogram can be considered as a discrete signal that can be processed by one of the traditional methods. You can, for example, get the spectrum of the rhythmogram. **Figure 8** shows the smoothed spectra of rhythmograms after low-frequency filtering. As can be seen, the signal S_2 spectrum stands out significantly compared to the signal spectra S_1 and S_3. For a quantitative assessment, we will perform a statistical analysis of rhythmograms. We calculate the mean, standard deviation, mode and median, as well as the minimum and maximum values. The calculated parameters are presented in **Table 1.**
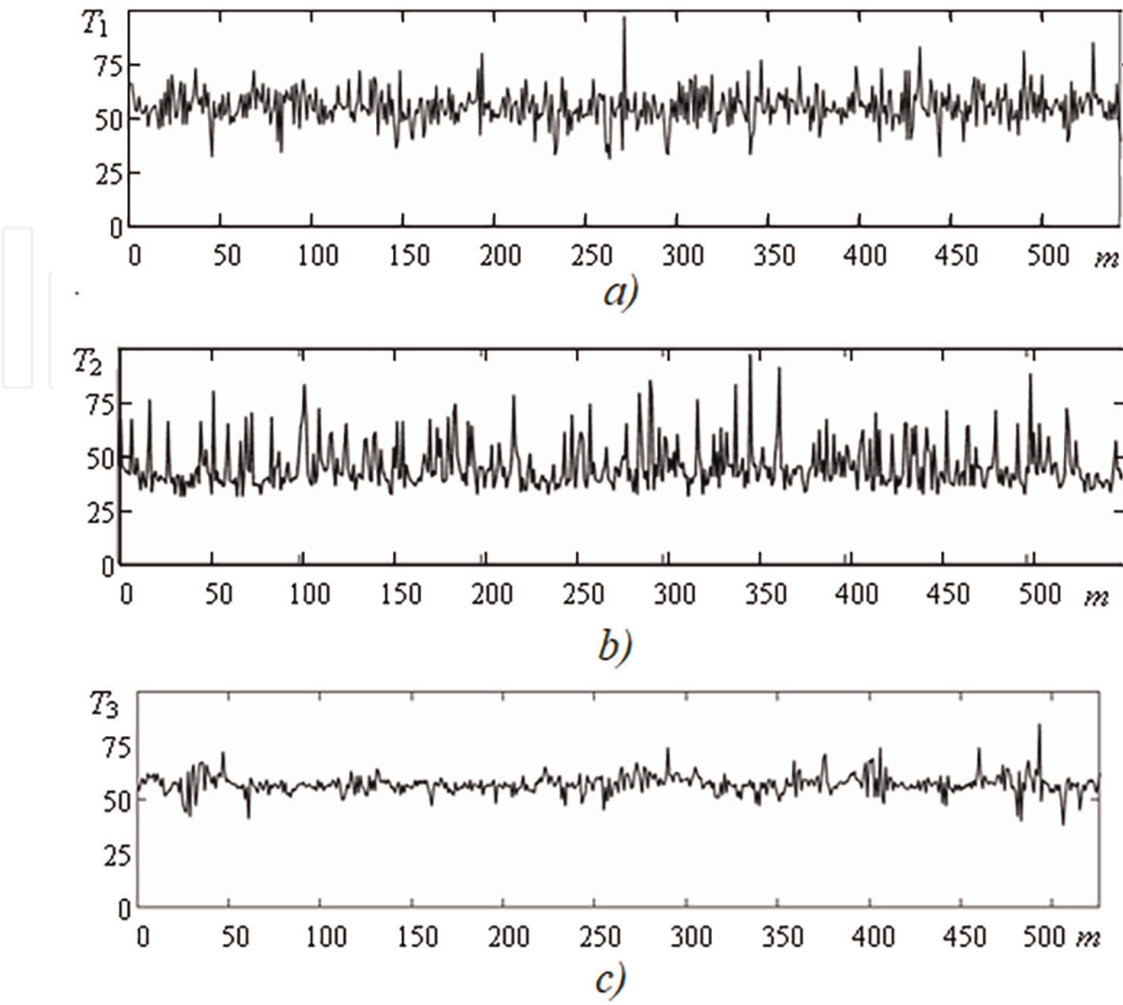
Figure 7.
Rhythmograms of signals, m is the number of the cross-correlation function maximum, T_1, T_2, T_3—the duration of the intervals between the maxima of the cross-correlation function.
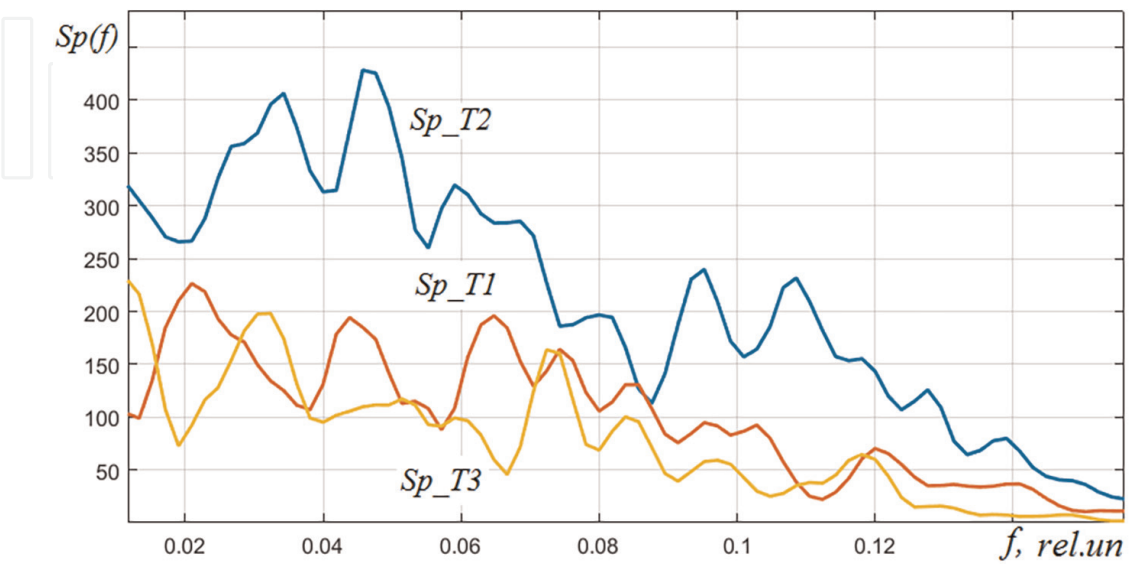

Figure 8.
Spectra of rhythmograms: Sp_T1—spectrum of T_1 rhythmogram, Sp_T2— spectrum of T_2 rhythmogram, Sp_T3— spectrum of T_3 rhythmogram.

Parameter	signal		
	S_1	S_2	S_3
Mean	55.2	47.5	55.9
Standard deviation	8.55	11.5	6.75
Median	54	44	56
Mode	52	43	56
Minimum value	32	31	32
Maximum value	101	109	88

Table 1.
Statistical parameters of rhythmograms.

In medical practice, the diagnosis of pathology is based on the value of standard deviation. The standard deviation values given in **Table 1** differ by 10%. The signal S_2 has the highest standard deviation value. The median and mode of recording signals S_1 and S_3 have close numerical values of the statistical parameters, which are close to the average. This indicates that the distribution of outliers relative to the mean value is close to symmetrical. For the signal S_2, downward surges (jerks and bumps) predominate. Next, consider the scatterograms of GTE bearing signals.

Scatterogram is a geometric method. In practice, the scatterogram has the shape of an ellipse stretched along the bisector **Figure 9** [12].
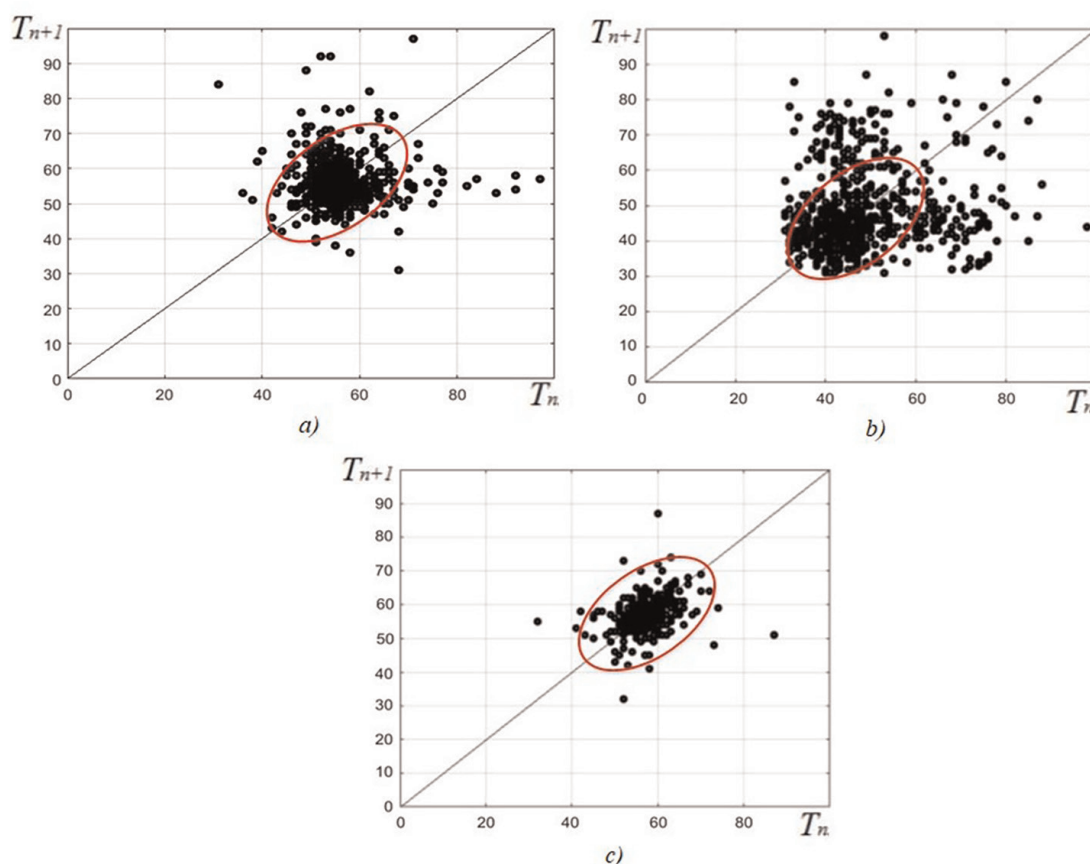

Figure 9.
Scatterograms of signals, Tn Tn + 1—duration of the previous and subsequent intervals between the maximum cross-correlation.

According to the scatterogram, one can judge the quasi-periodicity of the signal under study. The more clustered the points are, the less the quasi-periodicity.

The shift of the points to the right along the coordinate axis reflects a decrease in the rhythm, while the shift to the left reflects an increase. If the points are far from the whole population, then this may indicate a defect.

Based on the totality of statistical estimates of rhythmograms and the scatter of points in scatterograms, we can assume that the bearings S_1 and S_3 are both in good condition, and S_2—with a high degree of probability—are faulty.

2.3 Signal processing with a priori information

Next, consider the processing of vibration signals received from the stand SP-180 M (**Figure 10**). This bench allows you to test all sizes and types of modern and advanced bearings used in aircraft gas turbine engines. The rotational speed at the maximum mode of the inter-rotor and inter-shaft bearings installed between the shafts of the rotors of high and low pressure of the engine, rotating in the parallel direction, is 3000 rpm. Therefore, on the stand, the operation of the bearings is modeled at speeds from 0 to 3000 rpm [13].

Stand SP-180 M allows us to place sensors directly on the outer or inner rings of the bearing [14]. As a rule, it is installed by gluing on a non-rotating outer ring. The results obtained make it possible to judge the condition of the bearings by the generated vibrations measured by the vibration sensors (**Figure 11**).

GTE tests are also being carried out on the high-pressure rotor of which was prepared with additional vibration sensors on the high-pressure compressor support. The results obtained are compared with information from vibration sensors located on the outer casing of the engine (**Figure 12**).

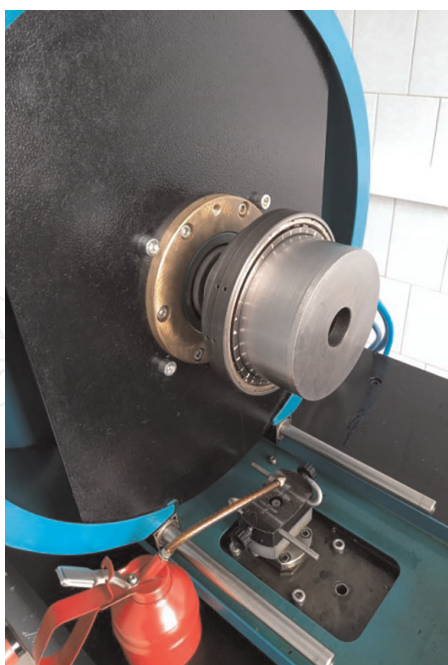**Figure 10.**
External view of the stand SP-180 M.

Figure 11.
Appearance of the installed bearing for vibration measurements by the built-in sensors of the bench.
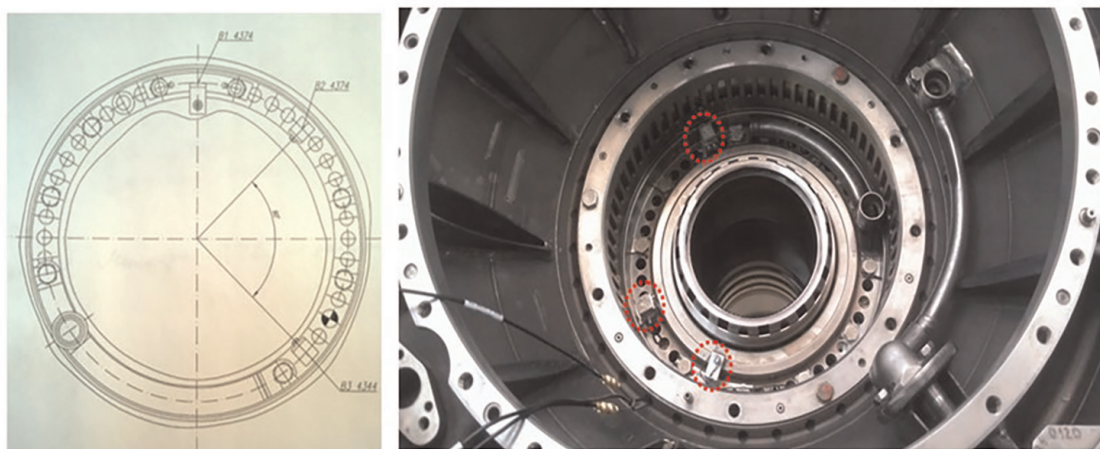

Figure 12.
Scheme and appearance of vibration sensors installed inside the engine, on the support of the GTE high-pressure compressor.

Figure 13 shows the fragments of vibration signals of the bearings received from SP-180 M. One bearing is good and the other two are defective. We will process the vibration signals using the above method.

From a priori information about the signals $S_1(t)$, $S_2(t)$, and $S_3(t)$, it is known that the rotation frequency of the separator is 23 Hz, the frequency of rotation of the rolling elements is 329 Hz, the frequency of rolling of the rolling elements along the outer ring is 529 Hz, and the frequency of rolling of the rolling elements along the inner ring is 612 Hz. In this regard, before selecting the standard, we will perform a preliminary filtering according to the scheme, which is shown in **Figure 14**.

In accordance with the scheme of **Figure 14**, the signal $S_1(t)$ of a healthy bearing is prefiltered, and each of the filters is a bandpass filter with the center frequency of the
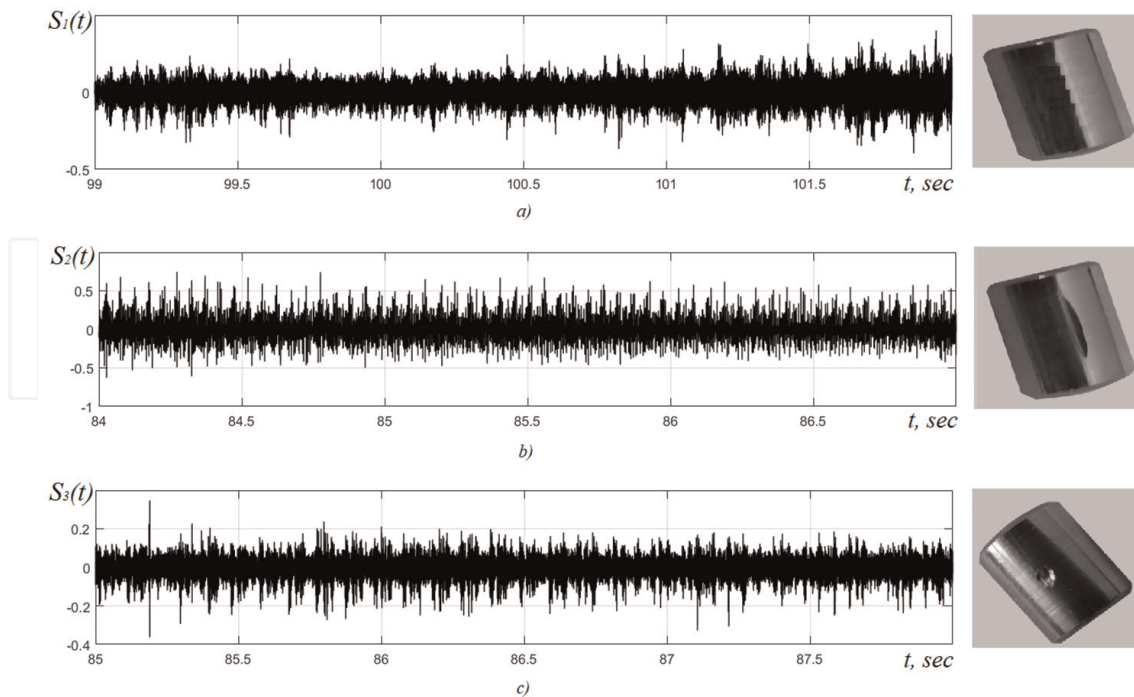
Figure 13.
Recordings of vibration signal of bearings: a) correct operation, b) damage—medium risk, and c) damage—point large and small.
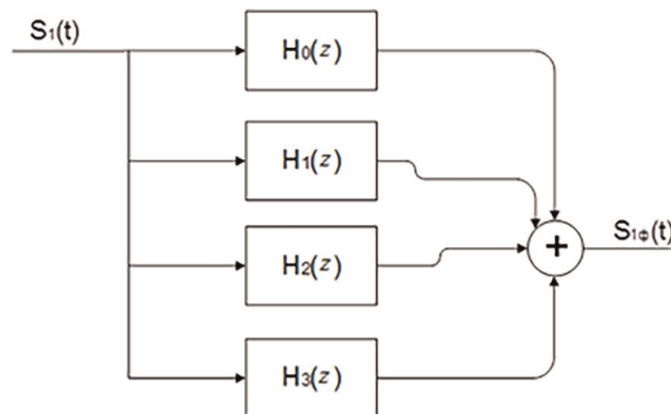

Figure 14.
Prefiltration scheme.

passband corresponding to the frequency component from the prior knowledge. It is also worth noting that the filtering procedure is performed separately, and the signal is summed at the output of each of the filters. The transfer coefficients of the bandpass filters are shown in **Figure 15**.

Next, a filter was designed according to the formula (7), the frequency response of which is shown in **Figure 16**. The frequency response peaks at the given a priori frequencies.

As a result, we have the following rhythmograms and scatterograms (**Figures 17** and **18**) and statistical evaluation **Table 2**.

Table 2 shows that the standard deviation value of the rhythmogram of a serviceable bearing is more than one and a half times lower than the standard deviation value of bearings with defects, which, in turn, can be an additional diagnostic feature.
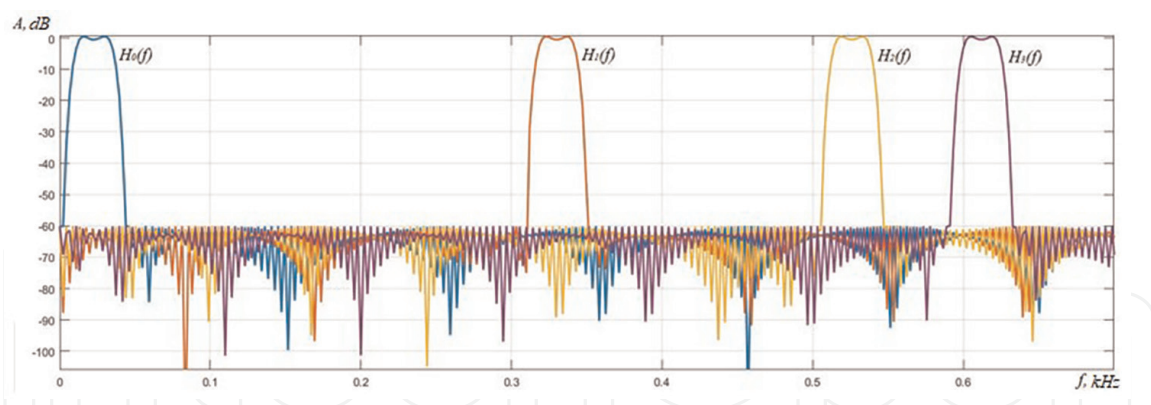
Figure 15.
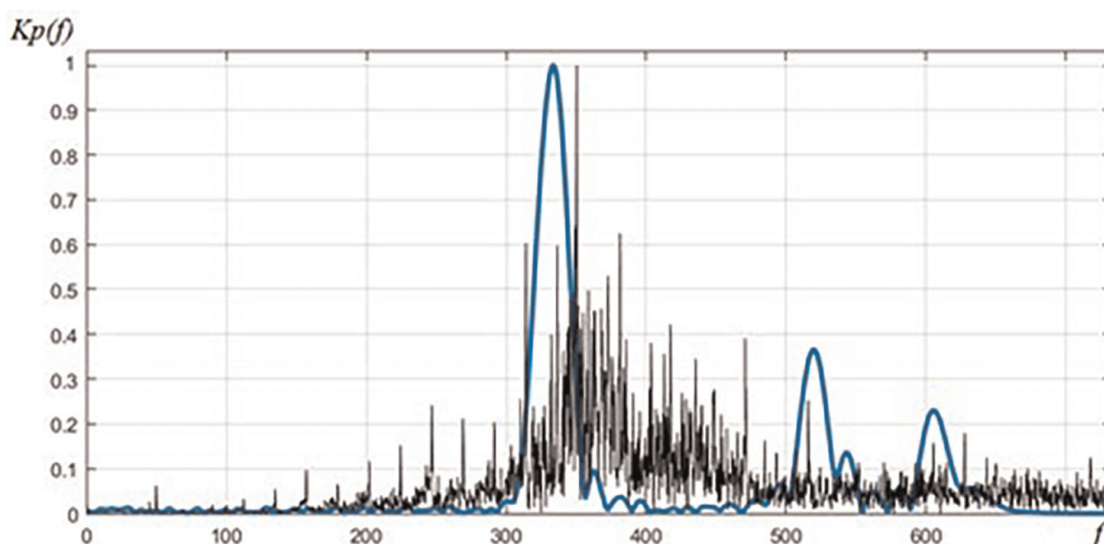*Frequency response of bandpass filters.*

Figure 16.
Quasi-matched filter and Fourier spectrum of a good bearing.

The median of the signal $S_1(t)$ record has a slight deviation from the numerical value of the mathematical expectation, while the deviation of the median from the average value for signals $S_2(t)$ and $S_3(t)$ above. An approximately similar picture is observed in the analysis of modes. This indicates that the distribution of outliers relative to the mean value is close to symmetric for $S_1(t)$. For signals $S_2(t)$ and $S_3(t)$ emissions down (jerks and bumps) prevail [15].

3. Conclusion

Rhythmogram and scatterogram allow you to explore the system in various modes, both standard and special. Therefore, it is able to provide additional diagnostic information about the state of the dynamic system. Thus, it can be hoped that such a diagnostic method may be of practical interest for assessing the characteristic dynamic features of the functioning of various mechanisms, devices, and apparatuses. Of course, the rhythmogram and the scatterogram will have a different look if another fragment of the record is chosen as a reference due to the change in SF. The issue of choosing a standard requires additional research with the involvement of diagnostic
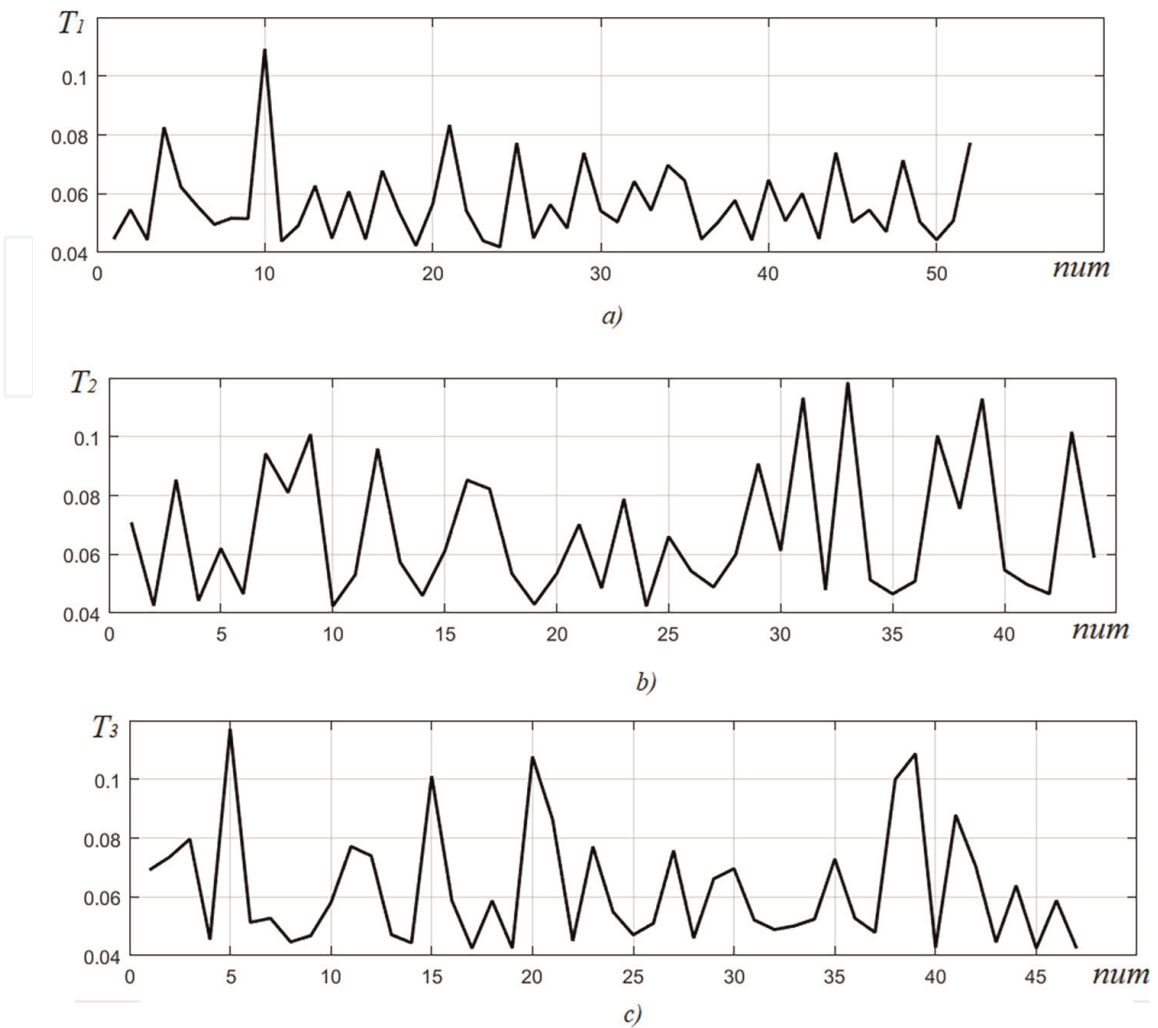
Figure 17.
Rhythmograms of signals num is the number of the maximum cross-correlation, T_1, T_2, T_3—the duration of the intervals between the maxima of the cross-correlation.

Parameter	Signal		
	$S_1(t)$	$S_2(t)$	$S_3(t)$
Mean	56.7	67.1	62.8
Standard deviation	13.3	22.3	20.1
Median	54	59.4	54.9
Mode	50.4	46.5	42.5
Minimum value	41.9	42.4	42.5
Maximum value	109.2	118.5	117.1

Table 2.
Statistical parameters of rhythmograms.

specialists in each specific case. The development of databases of various SF will allow for express diagnostics of devices. A feature of the method proposed and developed by us for processing quasi-periodic pulse signals using the Gauss-Hermite function is also
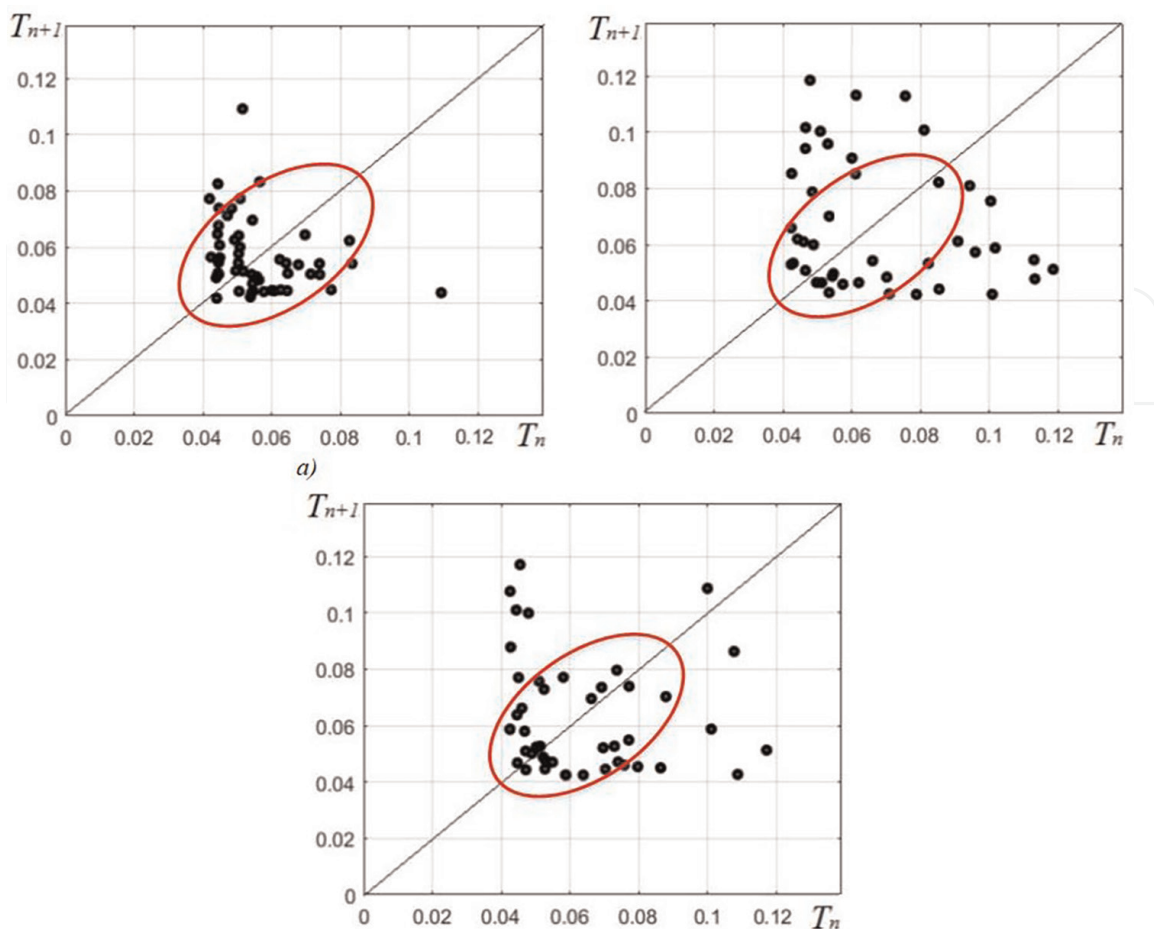
Figure 18.
Scatterograms of signals, Tn Tn + 1—duration of the previous and subsequent intervals between the maxima of the cross-correlation.

the possibility of varying the SF scale along the time axis. The scale variation makes it possible to detect not only violations of the system periodicity, but also a change in the shape of the signal pulses, which, in turn, provides additional means for detecting and predicting the development of a malfunction.

17

Author details

Dmitry Balakin[1*], Vitaly Shtykov[1], Alexey Zubko[2], Shalimova Elena Vladimirovna[1] and Zayed Saleh Salem Ali[1]

1 National Research University "Moscow Power Engineering Institute", Moscow, Russia

2 Moscow Aviation Institute (National Research University), Public Joint Stock Company «UEC-Ufa Engine Industrial Association» branch «OKB after A. Lyulki», Moscow, Russia

*Address all correspondence to: dabalakin@yandex.ru

IntechOpen

References

[1] Barkov AV, Barkova NA, Mitchell JS. Condition assessment and life prediction of rolling element bearings. Part 1. Sound and Vibration. 1995;**6**:10-17

[2] Adewusi S, Al-Bedoor BO. Wavelet analysis of vibration signals of an overhang rotor with a propagating transverse crack. Journal of Sound and Vibration. 2001;**246**(5):777-793. DOI: 10.1006/jsvi.2000.3611

[3] Chancey VC, Flowers GT. Identification of transient vibration characteristics using absolute harmonic wavelet coefficients. Journal of Vibration and Control. 2001;**11**(7):1175-1193. DOI: 10.1177/107754630100700803

[4] Peng Z, Chu F, He Y. Vibration signal analysis and feature extraction based on reassigned wavelet scalogram. Journal of Sound and Vibration. 2002;**253**(5): 1087-1100

[5] Nazolin AL. Possibility of detecting defects in the stator of Turbogenerator from the Spectrum of Vibroacoustic signal. Industrial laboratory. Diagnostics of materials. 2017;**83**(4): 49-54 (In Russ.)

[6] Sundukov AE, Sundukov EV. Analysis of the vibration state of quality bearings. Vestnik SSAU. 2006;**2**(10): 85-89 (In Russ.)

[7] Kostyukov VN, Naumenko AP. Handbook of Fundamentals of Vibroacoustic Diagnostics and Monitoring Ring of Machines. OmSTU Publishing House; 2011. p. 360 (In Russ.)

[8] Barkov AV, Barkova NA, Azovtsev AY. Handbook of Monitoring and Diagnostics of Rotary Machines by Vibration. SPbGMTU publishing house; 2000. p. 150 (In Russ.)

[9] Yurkevich VV. Diagnostics of rolling bearings. Stankoistroument. 2015;**1**: 97-99 (In Russ.)

[10] Martens JB. The Hermite transform: A survey. EURASIP Journal on Advances in Signal Processing. 2006;**2006**:026145

[11] Balakin DA. Construction of an orthogonal filter bank based on Hermite transforms for signal processing. Journal of Radio Electronics. 2014;**9**:8 (In Russ.)

[12] Balakin DA, Shtykov VV. Using rhythmograms to diagnose mechanical systems. In: Journal of Physics: Conference Series. IOP Publishing Ltd. Vol. 1399. APITECH; 2019. p. 4. DOI: 10.1088/1742-6596/1399/4/044027

[13] Semenova AS, Zubko AI. Studying technical condition of the interrotor bearing whith the SP-180M vibratory-diagnostic test bench after passing life tests. Vesnik of MAI. 2015;**26**(1):126-138 (In Russ.)

[14] Zubko AI. Complex Method of Vibrodiagnostics of the Technical Condition of Bearing Supports of Gas Turbine Engines [Thesis]. Moscow Aviation Institute: Moscow; 2020

[15] Balakin DA, Zubko AI, Zubko AA, Shtykov VV. Vibration diagnostics of rotor bearings, Hermite transformation, rhythmogram, scatterogram, quasi-periodicity. Vesnik of MAI. 2021;**28**(4): 151-162 (In Russ.)